OPEN ACCESS Freely available online

Journal of Geology & Geophysics

Research Article

Evaluation of the Quantitative Criteria of Triassic Carbonate Rocks Reservoirs

Sudad H Al-Obaidi[1*], Wj Chang[2]

[1]Department of Petroleum Engineering, Saint Petersburg Mining University, Saint Petersburg, Russia; [2]Department of Petroleum Engineering, University of Xidian, Xidian, China

ABSTRACT

South Mangyshlak basin is investigated in this paper. The Triassic deposits of carbonate rocks are investigated in this paper for their boundary values. These values are important for the interpretation of field geophysical data, as well as for perforation and blasting.

Triassic deposits, due to their lithological composition, are classified as either terrigenous or carbonate reservoirs. Carbonate reservoirs are found in the Middle Triassic strata containing volcanogenic dolomite and volcanogenic limestone rocks. These rocks create a complex type of reservoir that is characterized as porous-fractured, porous-cavernous, and fractured. The intercalation of tuffaceous, siltstone-sandy, and mudstone rocks create the Upper Triassic sediments which overlie Middle Triassic sedimentary rocks. Oil deposits are confined to polymictic sandstones, which are saturated with oil to varying degrees.

In order to substantiate the quantitative criteria of the reservoir, experimental studies of the core samples were conducted in the laboratory. Studies of fluid flow were conducted where physical and hydrodynamic characteristics were determined when oil was displaced by displacing reagents. Correlations between reservoirs and non-reservoirs were constructed based on the obtained parameters. The boundary values were determined based on relationships between reservoir properties, such as porosity and permeability versus residual water content, as well as effective porosity and permeability versus dynamic porosity. Using these results, the porosity limits for the Middle and Upper Triassic strata have been determined to be 7%, the permeability limits for the Middle Triassic have been determined to be 0.02×10^{-3} m^2, and the permeability limits for the Upper Triassic have been determined to be 0.3×10^{-3} m^2.

Keywords: Permeability; Effective porosity; Boundary values; Triassic deposits; Carbonate rocks reservoirs

INTRODUCTION

As a result of geological exploration at Mangyshlak basin during the 70s-90s of the last century, numerous oil and gas fields were discovered with proven productivity [1-4].Triassic carbonate reservoirs in the basin exhibit a number of characteristics, including complex pore structures, high heterogeneity in flow and reservoir properties, variety of rock compositions, and many others [5-8]. These characteristics complicate the interpretation of field geophysical data, the selection of reservoirs, and the design of development models.

Since the deposits have a complex structure and several factors that negatively affect the curves, it is difficult to identify the boundaries of carbonate reservoirs in Triassic deposits using well-logging methods when applying qualitative features. Therefore, the technology of identifying reservoirs according to quantitative criteria that determine the "reservoir-non-reservoir" boundary at the static level is necessary to clarify the interpretation [9-12]. In order to determine the boundary values, correlation dependencies were constructed based on the parameters obtained from special laboratory core tests.

Lithological and petrographic characteristics of Triassic carbonate reservoirs

Lower Triassic deposits (T1): The carbonate-terrigenous sequence of the Lower Triassic (T1), which lies at the base of the oil and gas complex, is composed of rhythmically interbedded siltstones, sandstones, mudstones, and limestones. Due to numerous ammonite finds in the carbonate-terrigenous sequence, the age of the carbonate-terrigenous sequence has been determined to be late Olenekian [13-15]. The reservoirs (porous-fractured) are

Correspondence to: Sudad H Al-Obaidi, Department of Petroleum Engineering, Saint Petersburg Mining University, Saint Petersburg, Russia, E-mail: drsudad@gmail.com

Received: 20-Jan-2022; Manuscript No. JGG-23-21475; **Editor assigned:** 23-Jan-2022; PreQC. No. JGG-23-21475 (PQ); **Reviewed:** 13-Feb-2023; QC. No. JGG-23-21475; **Revised:** 20-Feb-2023; Manuscript No. JGG-23-21475 (R); **Published:** 27-Feb-2023, DOI: 10.35248/2381-8719.23.12.1072.

Citation: Al-Obaidi SH, Chang W (2023) Evaluation of the Quantitative Criteria of Triassic Carbonate Rocks Reservoirs. J Geol Geophys. 12.1072.

composed of arkosic sandstones with effective porosity from 8 to 18%, fracture permeability up to 6.5 × 10^{-3} μm^2, and porous permeability from 0.1 to 141 × 10^{-3} μm^2 [16,17].

Middle Triassic deposits (T2): The Middle Triassic deposits (T2) consist of a volcanic-carbonate grey-colored formation, which accumulated under the conditions of a marine brackish-water basin and humid conditions. The formation consists of three lithological layers (from bottom to top):

- Volcanogenic-dolomitic
- Volcanogenic-limestone
- Volcanic-argillic

A volcanic-dolomite layer lies on the underlying Lower Triassic. The composition of this rock is characterized by the wide development of oolitic-cloddy tuffs, tuffites, tuff mudstones, and clastic polydetrital limestones. Due to the development of carbonate rocks, which can be easily leached, reservoir properties such as effective porosity and permeability are high. It has a porosity of up to 28% and a permeability of 115 × 10^{-3} μm^2 [18-20].

The void space is represented by intra-form isolated pores formed as a result of calcite leaching. The inter-formal space is filled with clear-crystalline calcite.

Immediately above the section is a volcanogenic limestone sequence, consisting of limestones with rare interlayers of dolomites, tuffites, tuff sandstones, mudstones and siltstones. The limestones are highly bituminized, which causes the black color of the rocks. There is a significant reduction in reservoir properties due to the widespread development of tuffaceous rocks.

The upper part of the Middle Triassic section-volcanogenic-argillite sequence is composed mainly of mudstones with an admixture of tuffaceous material and thin interlayers of carbonate rocks (lower part) and siltstones (upper part). The rocks are characterized by low reservoir properties and are often taken as a seal for hydrocarbon deposits confined to the carbonate layer [21,22].

Upper Triassic deposits (T3): There is a coarse-grained unit at the base of the stratum with a thickness of 40 m to 70 m with the following reservoir properties; effective porosity up to 20%, permeability of 10 × 10^{-3} μm^2 [23,24]. The overlying part of the section is composed of inequigranular tuff sandstones, tuff siltstones, and tuff mudstones [25,26].

The total thickness of the Middle Triassic deposits within the South Mangyshlak reaches 600 m-650 m [27,28].

MATERIALS AND METHODS

To assess the boundary values, studies were carried out on the selected core in the period 2010-2019 [29-30]. General information on sampling for the core studies is presented in Table 1.

Table 1: Detailed information about selected samples.

Field/ Well	Horizon	Lithology	Number of experiments
X-10	T3, Basal	Fine-grained sandstone	2
X-3	T3, Basal	Fine-grained sandstone	2
Y-9	T3, Basal	Tuff sandstone	2
Y-40	T3, Basal	Tuff sandstone	2
X-15	T2, volcanic-dolomitic	Calcareous dolomite	1
X-27	T2, volcanic-dolomitic	Clastic dolomite, cavernous	1
Y-40	T2	Tuff siltstone	1

To assess the boundary values of porosity and permeability properties, a 2-phase flow unit was used, the main elements of which are:

1. Vertically positioned core holder designed for core samples with a diameter of 1½ inches and a length of 12 inches.
2. Vertically positioned X-ray system for continuous core scanning and real-time determination of water-oil saturation.
3. A set of precision pumps and temperature sensors for fluid flow under thermobaric conditions.
4. Transducer module for differential pressure detection.

Preparation of core samples

The preparation of core samples for experimental studies included several stages.

Stage 1: Drilling samples with a diameter of 1½ inches were collected from the working part of the sawn core.

The resulting cylindrical samples were packed in plastic bags and sent to the extraction room for cleaning from hydrocarbons, formation water and salts. Samples were extracted in Soxhlet devices using toluene as a solvent [31-33], then a mixture of chloroform and methanol in a ratio of 9:1, respectively.

Purification completeness was determined in the process of daily monitoring by fluorescence in UV light as well as by weighing the samples after extraction and drying.

As soon as the cleaning process was complete, the samples were dried in a controlled humidity oven at 65°C until their weight reached a constant value.

Afterward, the samples were placed in a desiccator with silica gel to prevent the adsorption of moisture from the air and sent for standard and special core studies.

Stage 2: Matrix density, porosity, and absolute permeability were determined by standard core testing. To measure the matrix density of grains, coefficients of effective porosity, and absolute permeability of rocks, an UltraPoroPerm-500 device from Core Laboratories Instruments (CLI) was used [34,35].

The operating principle of the porosimeter is based on the use of the Boyle-Mariotte law. The gas volumetric method using helium was used to determine the matrix density and porosity of the samples. The porosity coefficient was calculated by the program as the ratio of the pore volume to the volume of the sample, with pore volume being the difference between sample volume and grain volume.

Absolute gas permeability was measured during steady-state flow using a standard Hassler core holder by injection of nitrogen gas. The operating principle of the permeameter is based on the use of Darcy's law [34,36]. A hydrostatic pressure of 400 psi was applied to the side surface of the sample. The absolute permeability of the rock was automatically calculated when the airflow followed the Darcy law.

Stage 3: In addition to the saturation of core samples using an auto-saturator with a reservoir water model, measurements were made of partial and residual water saturation coefficients,

relative phase permeability of oil and water, and residual oil saturation. Before the start of the experiments, the selected samples were saturated in a vacuum saturator with a Reservoir Water Model (RWM) using a prepared synthetic solution of the NaCl type with a mineralization of 20–40 g/l. A preliminary vacuum of the samples and saturating fluid was performed. In order to determine if the pore space is completely saturated, the porosity obtained by the saturation of the samples with RWM was compared with that calculated from the gas-volume method using helium. Crude-filtered oil was also prepared to saturate the core sample during the experiments.

The core samples, pre-saturated with RWM, were placed in a specially designed gamma-ray-transmitting core holder, where reservoir pressure was created. First, the water phase permeability of the rock was determined at 100% RWM saturation. Then, without removing the sample from the core holder, water was displaced under reservoir conditions using crude oil, and the coefficients of residual water saturation and oil phase permeability were determined. The coefficient of residual water saturation of core samples was determined from the results of X-ray scanning [37-39].

Steady-state studies

As soon as the core samples had been prepared, oil and water were injected simultaneously in different proportions: 75/1, 25/1, 5/1, 1/1, and 1/10. Each subsequent batch injection was performed after the stabilization of the differential pressure.

With the aid of an X-ray scanner, the effective permeability of each phase and water saturation of the samples were measured at each stage of the experiment.

After batch injection of two phases, water injection equal to 25 times the pore volume was performed until residual oil saturation was achieved, and oil phase permeability was determined.

The water saturation of the sample extracted from the core holder was also determined by the extraction method in the Dean-Stark apparatus [40-42].

To determine the oil phase permeability, the samples were additionally cleaned, dried, and saturated with crude oil. Then, the samples were placed in a core holder, after which crude oil was injected and the oil permeability coefficient was determined at 100% oil saturation.

The results of the experiments performed are presented in Table 2.

Table 2: Results of special core studies.

Indicators	Unit of meas.	Experiment							
		No 1	No 2	No 3	No 4	No 5	No 6	No 7	No 8
Field/well		X-10		X-3		Y-9		Y-40	
Laboratory no of the sample		26	22	5	7	225	242	219	220
Lithology		Sand-stone	Sand-stone	Sand-stone	Sand-stone	Tuff sandstone	Tuff sandstone	Tuff sandstone	Tuff sandstone
Depth	m	3256.2	3262.12	3699.54	3698.87	2962.03	3037.31	3703.05	3703.23
Effective porosity	Fraction	0.155	0.175	0.143	0.140	0.246	0.138	0.180	0.182
Absolute Permeability	$\times 10^{-3}$ μm^2	107.9	206.9	32.0	31.6	23.1	1.4	51.1	29.1
Density of formation water	g/cm3	1.056	1.056	1.056	1.056	1.061	1.061	1.061	1.061
Oil viscosity	mPa.s	0.560	0.560	0.560	0.560	1	1	1	1
Oil density	g/cm3	0.758	0.758	0.758	0.758	0.798	0.798	0.798	0.798
General mineralization	g/l	28	28	28	28	21	21	21	21
Residual water saturation	Fraction	0.220	0.230	0.276	0.262	0.384	0.470	0.334	0.391
Residual oil saturation	Fraction	0.356	0.325	0.349	0.355	0.345	0.349	0.366	0.351
Water permeability at residual oil	$\times 10^{-3}$ μm^2	5.676	5.860	8.022	7.977	6.545	0.216	17.556	5.470
Oil permeability	$\times 10^{-3}$ μm^2	13.583	13.292	4.920	5.687				

Oil permeability at residual water	× 10^{-3} μm^2	5.988	5.860	4.305	4.399	15.620	1.010	42.510	18.950
Oil displacement coefficient	Fraction	0.539	0.578	0.519	0.519	0.441	0.273	0.450	0.424
Experiment temperature	°C	130.6	130.6	130.6	130.6	115	115	115	115

RESULTS AND DISCUSSION

According to the results of the studies, Figure 1 presents graphs of relative permeability for both water and oil. The following conclusions can be drawn from these graphs of relative permeability:

1. Residual oil saturation of rocks varies within 32.5-36.6%.
2. Residual water saturation within 22.0-47.0%.
3. Oil displacement ratio is 27.3-57.8%.
4. The limiting value of the relative permeability of water is 0.2-0.4 units, indicating that the rocks are hydrophilic.

According to the results of special studies conducted, residual water saturation and oil saturation were determined.

The dynamic porosity of rocks was calculated using the following expression:

$$\varphi_D = \varphi_e * (1 - S_w - S_o) \quad \ldots (1)$$

Where:

φ_D-Dynamic porosity;

φ_e Effective porosity of rocks by helium;

S_w-Residual water saturation;

S_o-Residual oil saturation.

As the residual water-oil saturation is considered, the dynamic porosity characterizes the capacitive and flow properties of the formation. When the rock has a dynamic porosity of 0%, the residual water-oil saturations fill the entire pore space, making it a non-reservoir. It is possible to estimate the boundary values of Upper Triassic productive reservoirs using the constructed relationships "dynamic porosity-effective porosity" and "dynamic porosity-absolute permeability" presented in Figures 2 and 3.

Thus, the limit values for Upper Triassic reservoirs are defined as:

1. The porosity boundary value is 7%.
2. The value of the boundary permeability is 0.3 × 10^{-3} μm^2.

The Middle Triassic rocks were also studied in depth. Samples were taken from different wells and fields.

However, when performing studies for rocks from several fields, when water was injected, the differential pressure increased to 3200 psi, and the water permeability was less than 0.1 × 10^{-3} μm^2, which did not allow further studies. This factor may be related to the hydrophobicity of the rocks. A summary of the initial information and results can be found in Table 3.

For a more reliable determination of the hydrophobization of rocks, the most permeable laboratory sample No. 259A (63.7 × 10^{-3} μm^2), represented by calcareous dolomite, was chosen. The studies were carried out in a steady-state mode. The results are presented in Figure 4.

As a result of the relationship between the relative permeability of oil and water, we can conclude the following:

1. Residual oil saturation of rocks is high-46.4%;
2. Residual water saturation-27.0%;
3. Oil displacement ratio is only 36.4%;
4. The limiting value of the water's relative permeability is 0.83 units, which indicates the hydrophobicity of the rocks.

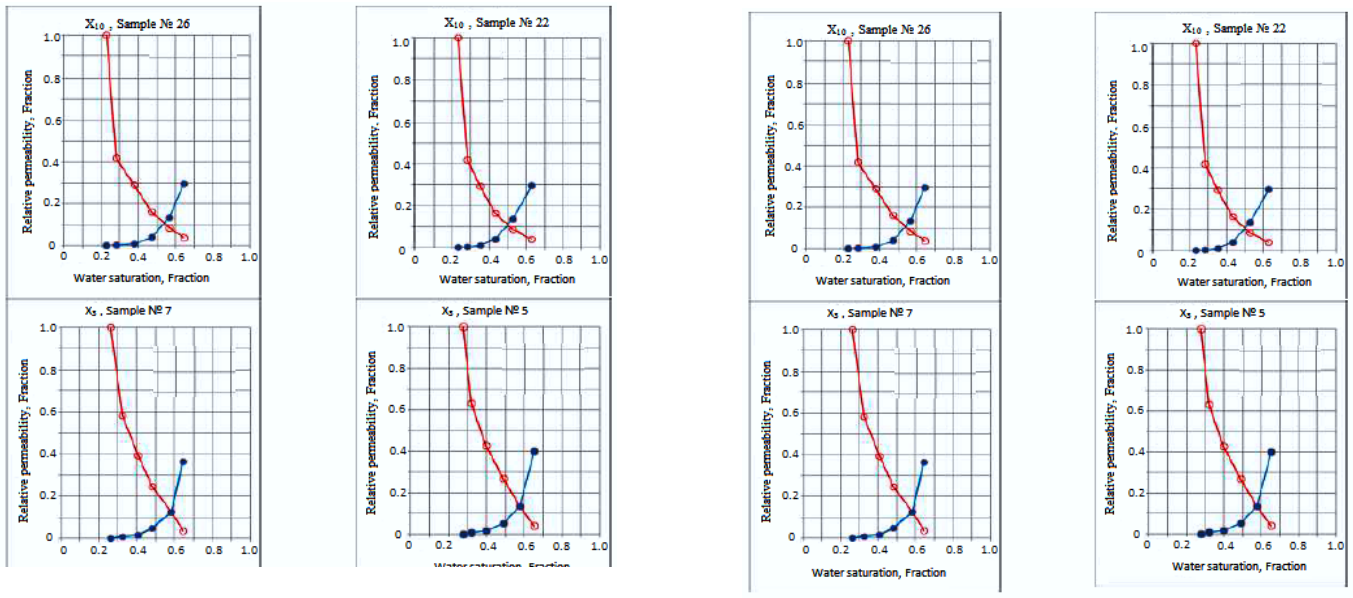

Figure 1: The relative permeability curves for oil and water. **Note:** (—●—) K_{ro}, (—●—) K_{rw}.

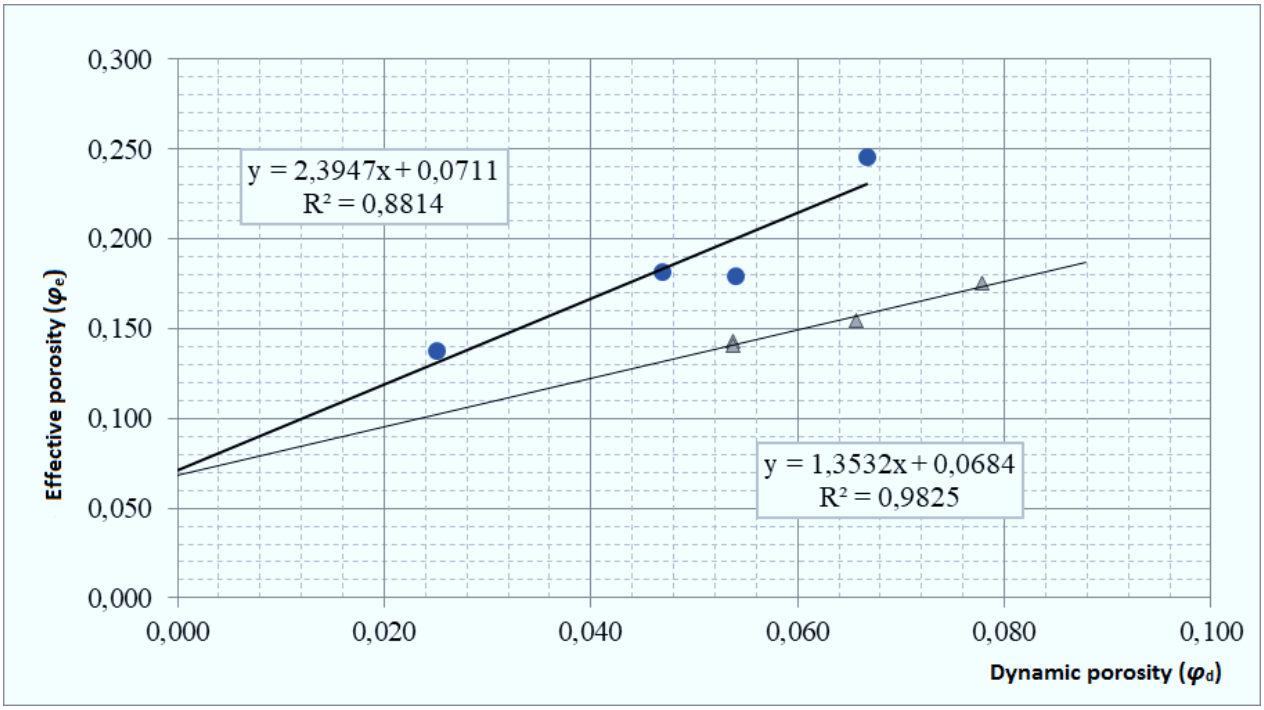

Figure 2: The relationship between dynamic porosity and effective porosity. **Note:** (●) Samples from wells Y9, Y40, (▲) Samples from wells X3, X10.

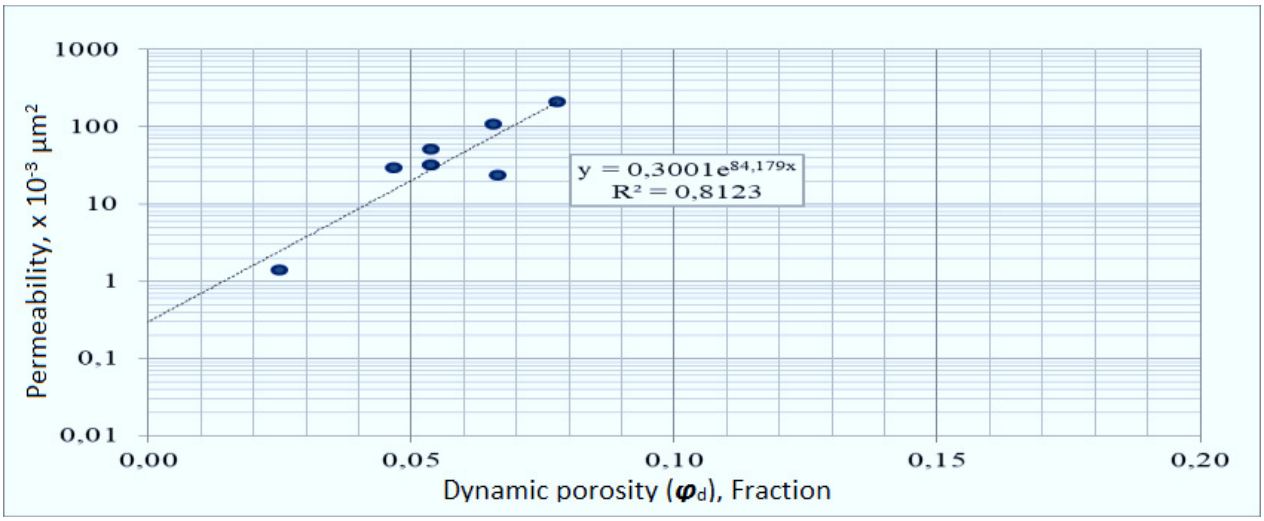

Figure 3: The relationship between dynamic porosity and absolute permeability.

Table 3: Results of special core studies.

Indicators	Unit of measurement	Experiment		
		No 5	No 6	No 7
Field/well		X-15	X-27	Y-40
Laboratory no of the sample		259A	161	2
Lithology		Calcareous dolomite	Dolomite	Tuff siltstone
Depth	m	2944.91	3789.55	3588.31

Effective porosity	Fraction	0.237	0.153	0.103
Absolute permeability	× 10^{-3} μm^2	63.7	0.63	0.237
Density of formation water	g/cm^3	1.061	1.06	1.061
Oil viscosity	mPa.s	1	1	1
Oil density	g/cm^3	0.798	0.8	0.798
General mineralization	g/l	24.5	21	21
Residual water saturation	Fraction	0.27038	0.453	0.35
Residual oil saturation	Fraction	0.464	-	-
Oil permeability	× 10^{-3} μm^2	4.81	0.11	0.05
Oil permeability at residual water	× 10^{-3} μm^2	3.76	-	-
Oil displacement coefficient	Fraction	0.364	-	-
Experiment temperature	°C	115	115	115

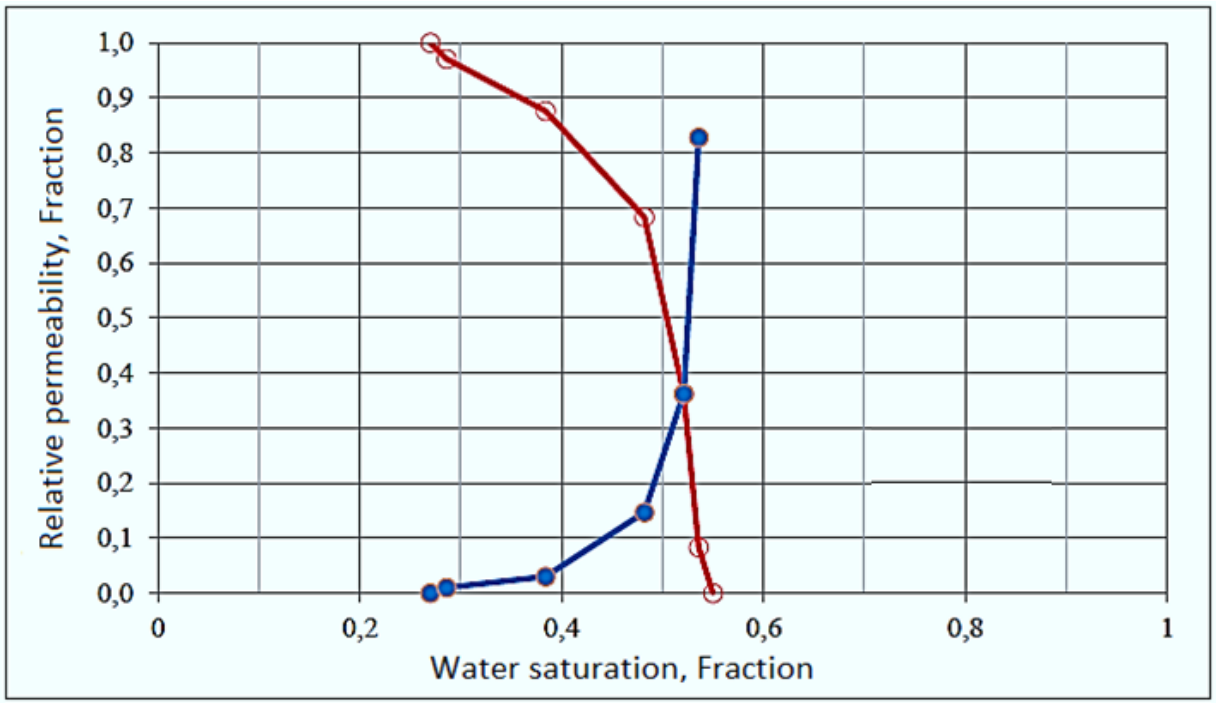

Figure 4: The relative permeability curves for oil and water. **Note:**) K_{ro}, ( ) K_{rw}.

To determine the boundary value of the effective porosity of rocks, instead of determining the residual oil saturation and, accordingly, dynamic porosity, a mass determination of capillary pressure was performed under reservoir conditions using a high-speed centrifuge.

The studies involved 124 samples selected in 2012-2015 [43-45]. A maximum capillary pressure of 215 psi was used to determine residual water saturation. The obtained values of residual water saturation are compared with effective porosity. The dependencies are shown in Figures 5 and 6.

According to the constructed dependencies, it can be seen that with a residual water saturation of more than 35%, the reservoir properties of rocks deteriorate, the fluid occupies the entire pore space, and the rock becomes a non-reservoir.

Thus, the defined limit values for volcanic-carbonate rocks of the Middle Triassic are as follows:

1. The porosity boundary value is 7%.

2. The value of the boundary permeability is 0.02 × 10^{-3} μm².

The reliability of reservoir properties determination in the course of well-logging data interpretation depends on the reliability of established petro-physical relationships and parameters. The quality of the core analysis carried out in the 80s does not allow today to use the results of these analyzes to build petro-physical relationships for the following reasons:

1. A low level of core recovery.
2. The lack of results from the profile studies intended to link the core to the rock section.
3. Lack of uniform sampling of cylindrical samples from all intervals, including low-permeability and non-reservoirs.
4. Insufficiency of studies-the lack of a set of studies on the same samples to establish the closeness of relationships between various parameters.

Consequently, the selection of cores and the study of reservoir properties of rocks should be continued.

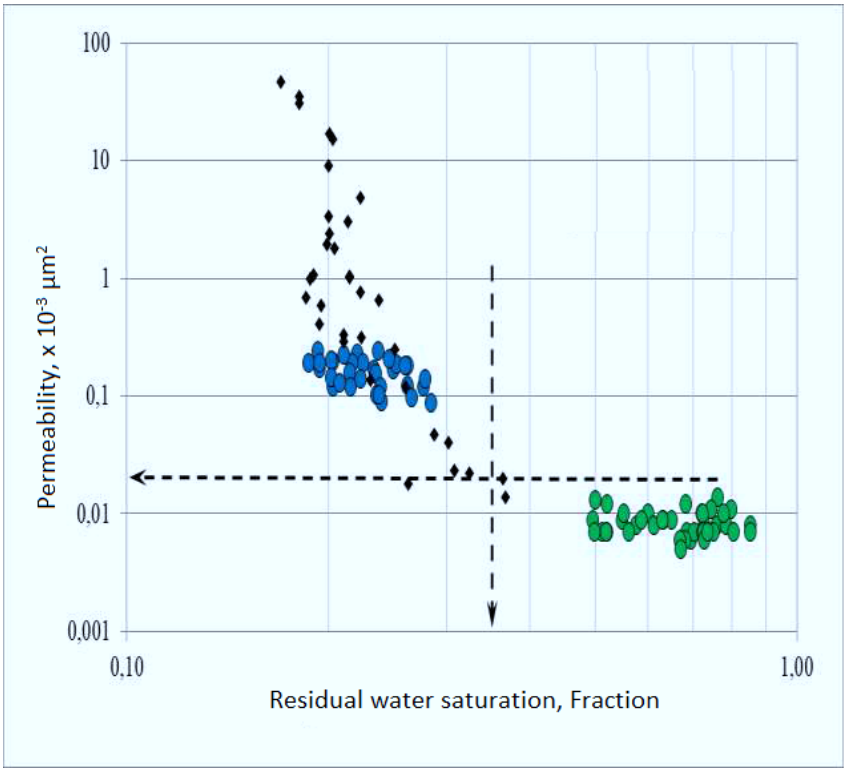

Figure 5: The relationship between the absolute permeability and residual water saturation. **Note:** A samples from the wells X10, X3, B samples from the wells Y9, Y40, C samples from other wells.

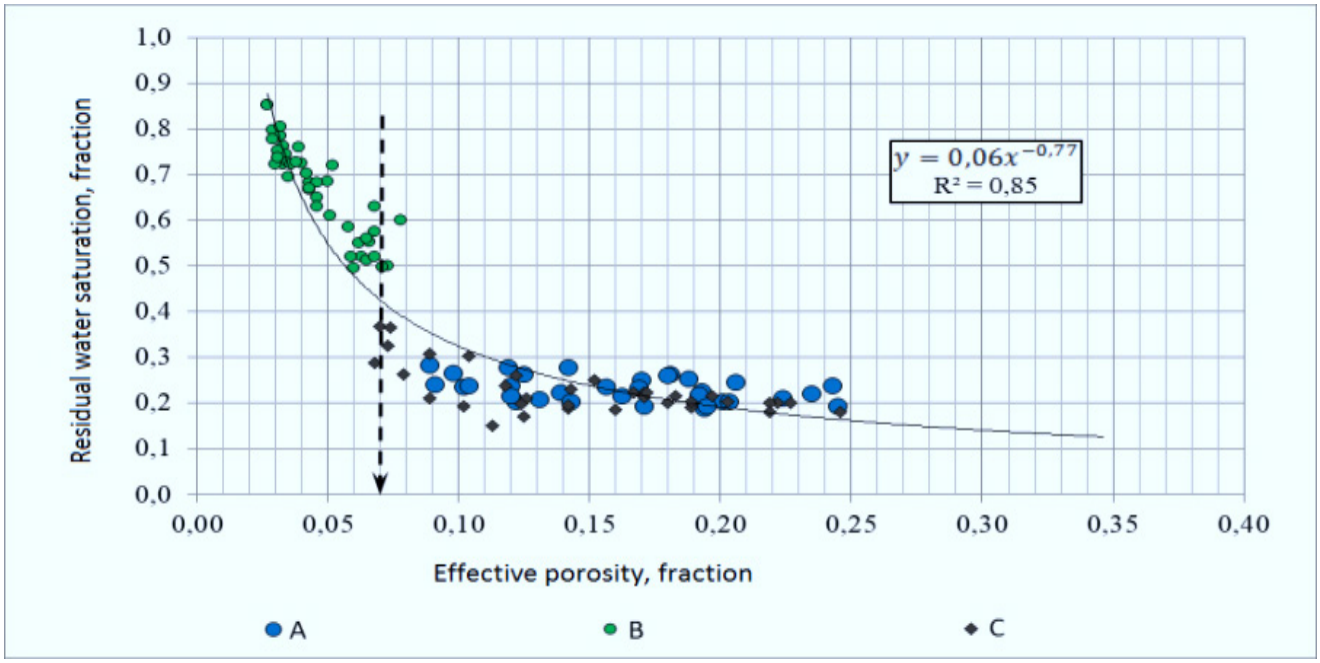

Figure 6: The relationship between the effective porosity and residual water saturation. **Note:** A samples from the wells X10, X3, B samples from the wells Y9, Y40, C samples from other wells.

CONCLUSION

Experimental analyses of the core samples were conducted in the laboratory in order to substantiate the quantitative criteria of the reservoir. By analyzing the parameters, correlations were constructed between reservoirs and non-reservoirs. Boundary values were determined by analyzing the relationships between reservoir properties, such as porosity and permeability, and residual water content. Based on the results of this work, the porosity limits for the Middle and Upper Triassic strata are 7%, the permeability limits for the Middle Triassic are 0.02×10^{-3} μm^2, and the permeability limits for the Upper Triassic are 0.3×10^{-3} μm^2. The use of the obtained boundary values contributes to the identification of complex carbonate reservoirs using both qualitative and quantitative features based on the difference in reservoir properties of reservoir rocks and host rocks. Since cores are being taken from new wells and various fields, the study of boundary values needs to be continued.

REFERENCES

1. Krupin AA, Rykus MV. Oil and gas potential of secondary hydrocarbon reservoirs in carbonate rocks of the Middle Triassic at the South Mangyshlak Fields. Oil Gas Business. 2012; (3):276.
2. Miel H, Hameed AO, Hussein KF. Modeling and monitoring the development of an oil field under conditions of mass hydraulic fracturing. Trend Sci. 2022;19(8):3436.
3. Murzagaliev DM. Rifting and petroleum productivity of Mangyshlak. Geol Nefti Gaza. 1996;(5):36-39.
4. Kamensky IP, Al-Obaidi SH, Khalaf FH. Scale effect in laboratory determination of the properties of complex carbonate reservoirs. Int Res J Mod Eng Technol Sci. 2020;2(11):1-6.
5. Sobornov KO. Geologic framework of the petroleum productive thrust belt of eastern Caucasus. Geol Nefti Gaza. 1995;(10):16-21.
6. Al-Obaidi SH, Khalaf FH, Smirnov VI. New technologies to improve the performance of high water cut wells equipped with ESP. Technium. 2020;3(1):104-113.
7. Timurziev AI. 1984. Characteristics of reservoir rocks and hydrocarbonpools in low permeable sections and improvement of methods for their prediction. Geol Nefti Gaza. 1984;(11):49-54.
8. Al-Obaidi SH, Khalaf FH. Acoustic logging methods in fractured and porous formations. J Geol Geophys. 2017;6(4):2.
9. Orudzheva DS, Popkov VI, Rabinovich AA. New data on the geology and petroleum potential of pre-Jurassic rocks of SouthMangyshlak, Geol Nefti Gaza. 1985;(7):17-22.
10. Al-Obaidi SH, Kamensky IP, Hofmann M. Changes in the physical properties of hydrocarbon reservoir as a result of an increase in the effective pressure during the development of the field. engrXiv. 2010.
11. Petersilie VI, Poroskuna VI, Yatsenko GG. Guidelines for calculating the geological reserves of oil and gas by the volumetric method, VNIGNI, NPC Tvergeofizika. Moscow-Tver. 2003:246:3-17.
12. Al-Obaidi SH, Khalaf FH. The Effect of anisotropy in formation permeability on the efficiency of cyclic water flooding. Int J Sci Technol Res. 2017;6(11):223-226.
13. Ulmishek GF. Petroleum geology and resources of the Middle Caspian Basin, former Soviet Union. US Department of the Interior, USGS. 2001.
14. Al-Obaidi S. Investigation of rheological properties of heavy oil deposits. In Advances in Geophysics, Tectonics and Petroleum Geosciences: Proceedings of the 2nd Springer Conference of the Arabian Journal of Geosciences (CAJG-2), Tunisia 2019. Springer. 2022;399-402.
15. Obaidi SH, Khalaf FH. Prospects for improving the efficiency of water insulation works in gas wells. J Geol Geophys. 2020;9(6):483.
16. Rabinovich AA, Palamar VP, Popkov VI. Basic principles of formation of oil and gas deposits, Nauka, Moscow. UDC. 1983;553.
17. Chang WJ, Al-Obaidi SH, Patkin AA. Assessment of the condition of the near-wellbore zone of repaired wells by the skin factor. Int Res J Mod Eng Tech Sci. 2021;3:1371-1377.
18. Gurbanov VS. Lithostratigraphic characteristic and lithology of triassic–paleozoic rocks of Southern Mangyshlak. Lithol Mineral Resour. 2004;39(6):541-554.
19. Al-Obaidi SH. Analysis of hydrodynamic methods for enhancing oil recovery. J Petrol Eng Technol. 2021;6:20-26.
20. Kettanah YA. Book Review: Energy Sources. Taylor Francis. 2003;25(11):1113-1117.
21. Al-Obaidi SH, Patkin AA, Guliaeva NI. Advance Use for the NMR relaxometry to investigate reservoir rocks. J Petrol Eng Technol. 2003;2(3):45-48.
22. Smirnov VI, Al-Obaidi Sudad H. Innovative methods of enhanced oil recovery. Oil Gas Res. 2008;1(e101):1.
23. Zholtayev GZ, Kuandykov BM. Geodynamic structural model of the south of Eurasia. Oil Gas. 1999;(2):62-74.
24. Al-Obaidi SH, Kamensky IP. Express study of rheological properties and group composition of oil and condensate using nuclear magnetic resonance–relaxometry. J Oil Gas Coal Technol. 2022;4(1):102.
25. Al-Obaidi S, Galkin A. Dependences of reservoir oil properties on surface oil. J Petrol Eng Emerg Technol. 2005;5:74-77.
26. Al-Obaidi S, Galkin A, Patkin A. Prospects of high viscosity oil flow rate in horizontal wells. J Petrol Eng Technol. 2006;5(4):56-62.
27. Kurmanov S. Carbonate sediments of the pre-Caspian Basin. Geol Kazakhstan. 1999;(4):67-76.
28. Al-Obaidi SH, Hofmann M, Smirnov VI, Khalaf FH, Alwan HH. Study of compositions for selective water isolation in gas wells. Nat Sci Adv Technol Edu. 2021;30(6).
29. Al-Obaidi SH. Improve the efficiency of the study of complex reservoirs and hydrocarbon deposits-East Baghdad Field. Int

J Sci Technol Res. 2016;5(8):129-131.

30. Al-Obaidi SH, Guliaeva NI, Smirnov VI. Influence of structure forming components on the viscosity of oils. Int J Sci Technol Res. 2020;9(11):347-351.
31. Patkin A, Al-Obaidi S. Influence of temperature and pressure of incoming oil-containing liquid from field wells on the gas separation process. J Petrol Eng Emerg Technol. 2001;3(4):20-24.
32. Shilanov NS. Evaluation of the oil and gas potential of the Triassic-Paleozoic deposits of the South Mangyshlak on the basis of complex data of geological and geophysical studies. Dissertation for the degree of Doctor of Philosophy in Earth Sciences, Baku. 2018:p102.
33. Al-Obaidi SH, Khalaf FH. Development of traditional water flooding to increase oil recovery. Int J Sci Tech Res. 2019;8:177-181.
34. Abitova AZ, Altimirov TZ, Shilanov NS. Standard and special laboratory studies of core. KazNIPImunaigas. 2013;(1):39-162.
35. Al-Obaidi SH, Kamensky IP, Smirnov VI. Investigation of thermal properties of reservoir rocks at different saturation. engrXiv. 2020.
36. Al-Obaidi SH. Comparison of different logging techniques for porosity determination to evaluate water saturation. engrXiv. 2020.
37. AL-Obaidi SH, Wj C, Hofmann M. Modelling the development of oil rim using water and gas injection. Nat Sci Adv Technol Edu. 2022;31(3).
38. Joseph J, Gunda NS, Mitra SK. On-chip porous media: Porosity and permeability measurements. Chem Eng Sci. 2013;99:274-283.
39. Al-Obaidi SH, Guliaeva NI. Determination of flow and volumetric properties of core samples using laboratory NMR relaxometry. J Petrol Eng Technol. 2002;1(2):20-23.
40. Nijp JJ, Metselaar K, Limpens J, Gooren HP, van der Zee SE. A modification of the constant-head permeameter to measure saturated hydraulic conductivity of highly permeable media. MethodsX. 2017;4:134-142.
41. Al-Obaidi SH, Chang WJ, Khalaf FH. Determination of the upper limit up to which the linear flow law (Darcy's Law) can be applied. J Xidian University. 2021;15(6):277-286.
42. Withjack EM, Devier C, Michael G. The role of X-ray computed tomography in core analysis. In SPE Western Regional/AAPG Pacific Section Joint Meeting. OnePetro. 2003.
43. Al-Obaidi SH, Kamensky IP, Hofmann M, Khalaf FH. An Evaluation of water and gas injections with hydraulic fracturing and horizontal wells in oil-saturated shale formations. Nat Sci Adv Technol Edu. 2022;31(4).
44. Handwerger DA, Willberg D, Pagels M, Rowland B, Keller JF. Reconciling retort versus dean stark measurements on tight shales. In SPE Annual Technical Conference and Exhibition. OnePetro. 2012.
45. Chang WJ, Al-Obaidi SH, Patkin AA. The use of oil-soluble polymers to enhance oil recovery in hard to recover hydrocarbons reserves. Int Res J Mod Eng Technol Sci. 2021;3(1):982-987.